Journal of Solid State Chemistry **154,** 384–389 (2000)
doi:10.1006/jssc.2000.8799, available online at http://www.idealibrary.com on IDEAL®

A Theoretical Investigation of Bonding and Electron Counting in Compounds Structurally Related to Ti_5Te_4

Mounir Bouayed,* Hassan Rabaâ,* Albert Le Beuze,† Stéphanie Députier,† Roland Guérin,† and Jean-Yves Saillard†,[1]

*Laboratoire de Chimie Théorique, Université Ibn Tofail, BP 133, 14000 Kénitra, Maroc; and †LCSIM-UMR 6511, Institut de Chimie de Rennes, Université de Rennes 1, 35042 Rennes Cedex, France

Received March 28, 2000; in revised form May 30, 2000; accepted June 16, 2000; published online September 30, 2000

Extended Hückel tight-binding calculations indicate that the valence electron count (VEC) of compounds adopting the Ti_5Te_4-type structure is imposed by metal–metal bonding. The average metal–metal overlap population is almost constant and maximum in the VEC range 44–50, which corresponds exactly to the VEC range of the characterized compounds. Related phases deriving from the Ti_5Te_4 structure through insertion of extra metal atoms or metal clusters between the chains have very similar bonding and VEC count. Calculations on V_3As_2 and $Cu_4Nb_5Si_4$ indicate that the inserted atoms provide Ti_5Te_4-type substructure with an electron number, which tends to maximize the metal–metal bonding. © 2000 Academic Press

Key Words: **band-structure calculations; Ti_5Te_4-type structure.**

INTRODUCTION

Recently some of us prepared $W_5As_{2.5}P_{1.5}$ (1), which is the latest member of a growing family of compounds having the tetragonal $I4/m$ Ti_5Te_4-type structure (1–12) which are reported in Table 1. In this compound, the W atoms form distorted (D_{4h}) octahedra, triangular faces of which are capped by pnictide atoms. The As and P atoms are fully disordered and simply labeled as As atoms in the following. The resulting W_6As_8 units are arranged in such a way that each of them shares two *trans* W atoms with its two neighbors, giving rise to the formation of W_5As_4 columns running parallel to the c axis, as shown in Fig. 1. The W_5As_4 columns are linked together through W–As and W–W contacts.

As shown in Table 1, the valence electron count (VEC) per M_5X_4 unit (M = transition metal, X = nonmetal) of such compounds varies from 44 to 50, suggesting that the stability of this architecture allows a small range of electron counts.

[1] To whom correspondence should be addressed. Fax: 33 2 99 38 34 87. E-mail: saillard@univ-rennes1.fr.

In the Ti_5Te_4-type structure, metalloid voids are present between neighboring chains. In some related compounds, these voids are occupied by a single metal atom, as in V_3As_2 (VV_5As_4) (10) where the inserted V atoms lies in an octahedral environment of arsenic, as shown in Fig. 2. In other compounds such as $Ni_4Nb_5P_4$ (11,12) or $Cu_4Nb_5Si_4$ (13), the M_5X_4 chains are able to free larger voids that can be filled by M'_4 tetrahedra. These tetrahedra are fused through condensation of opposite edges, thus forming columns which run parallel to the M_5X_4 ones, as shown in Fig. 3. In these structures, the M' atoms are surrounded by three X atoms in a distorted trigonal planar disposition.

In this paper we investigate the electronic structure of W_5As_4 in order to analyze the bonding in the M_5X_4 series and to answer the question as to the stability of these compounds with respect to their VEC. One other important question we address concerns the role played by the inserted atoms or clusters in the stability of the stuffed M_3X_2 (MM_5X_4) and $M'_4M_5X_4$ phases. Do they only strengthen the crystal cohesion by filling the voids and creating supplementary links between the M_5X_4 columns, or do they behave as electron–donor or electron–sink systems with respect to the M_5X_4 framework in order to adjust its VEC to a favorable value.

COMPUTATIONAL DETAILS

All the calculations are of the extended Hückel type (14, 15) and carried out within the tight-binding formalism (16, 17), which takes into account the periodical nature of the extended structures. The calculations were performed by using the YAEMOP package (18), which provides *inter alia* useful graphical outputs such as band structures, densities of states (DOS), and crystal orbital overlap population (COOP) curves (19). A COOP curve represents the variation of the overlap population between two atoms with respect to the energy. It is indicative of the strength and the nature of a particular interatomic interaction: A positive

0022-4596/00 $35.00

TABLE 1
Compounds Adopting in Ti_5Te_4-Type Structure and Compounds Having Related Structures

Compound (ref.)	VEC
Ti_5Te_4 (2)	44
V_5Sb_4 (3)	45
Nb_5Sb_4 (6)	45
Ta_5Sb_4 (8)	45
V_5S_4 (4)	49
V_5Se_4 (5)	49
Nb_5Se_4 (7)	49
Nb_5Te_4 (7)	49
Mo_5As_4 (9)	50
$W_5As_{2.5}P_{1.5}$ (1)	50
$V_3As_2(VV_5As_4)$ (10)	47.5[a]
$Ni_4Nb_5P_4$ (11)	45[a]
$Ni_4Ta_5P_4$ (12)	45[a]
$Cu_4Nb_5Si_4$ (13)	45[a]

[a] VEC evaluated from the band-structure calculations (see text).

value means a bonding interaction, while a negative value means a repulsive interaction. The horizontal scales of the COOP curves shown in this paper are all arbitrary. Each of the valence atomic orbitals (AOs) was described by one Slater-type orbital (STO), except for the metal *d*-type AOs, which were described by a linear combination of two STOs. All the atomic parameters used in the calculations are standard values taken from the literature (20). They are listed in Table 2. The experimental X-ray structures were always considered.

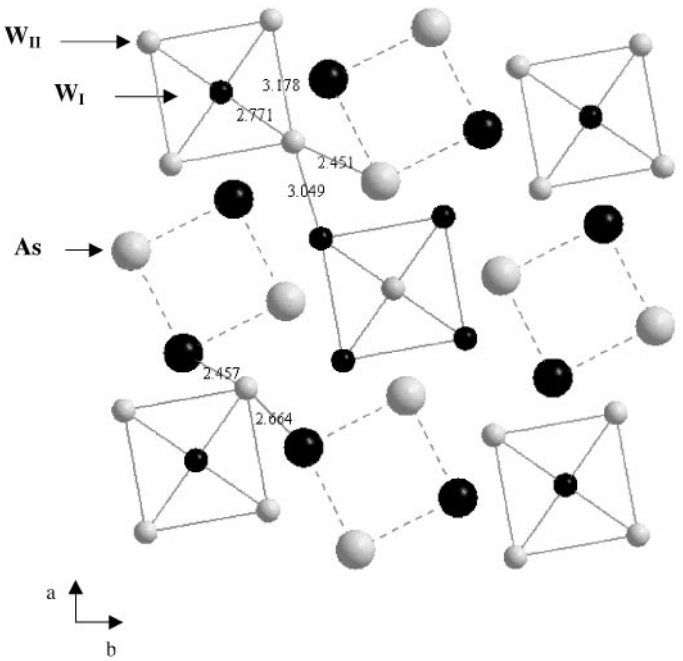

FIG. 1. Projection on the (001) plane of the $W_5As_{2.5}P_{1.5}$ structure. The pnictide sites are randomly occupied by As and P and are labeled As.

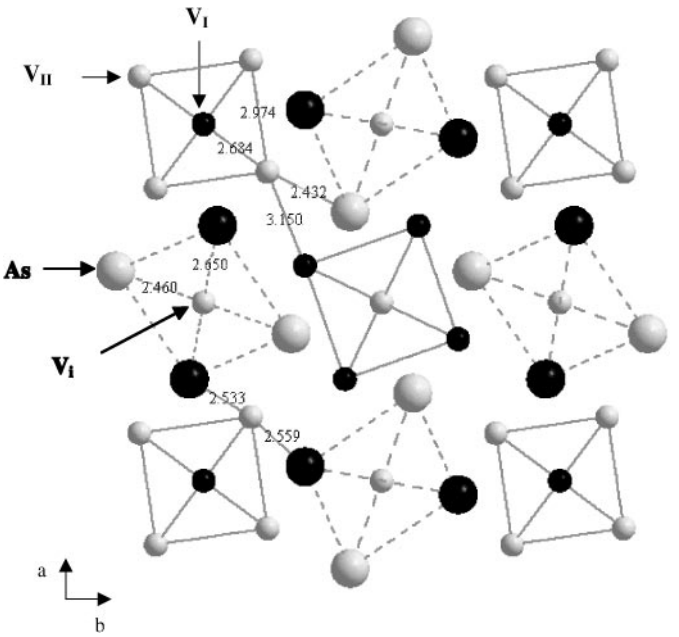

FIG. 2. Projection on the (001) plane of the V_3As_2 (VV_5As_4) structure.

BONDING ANALYSIS OF THE W_5As_4 MODEL

The stoichiometric W_5As_4 compound was chosen to model $W_5As_{2.5}P_{1.5}$. Its band structure is shown in Fig. 4. It clearly shows a metallic character. The bands associated to

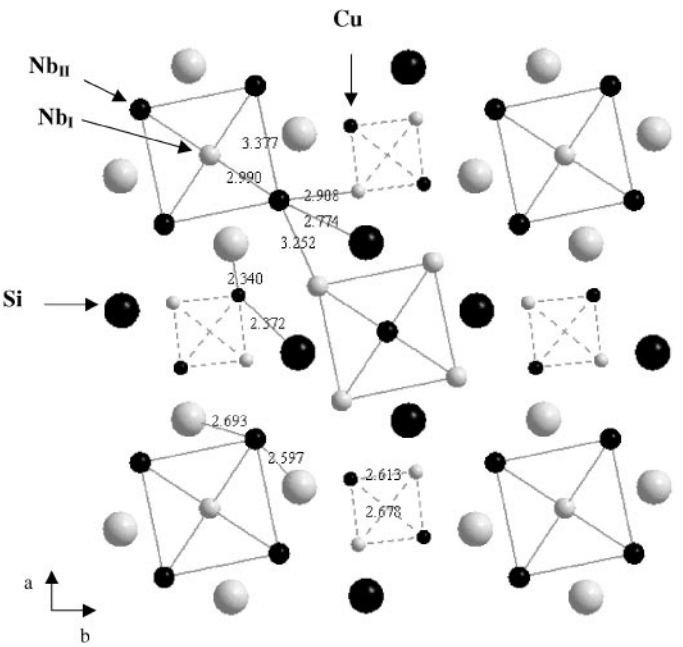

FIG. 3. Projection on the (001) plane of the $Cu_4Nb_5Si_4$.

TABLE 2
Extended Hückel Atomic Parameters Used in the Tight-Binding Calculations

Atom	Orbital	H_{ii} (eV)	$\zeta_1{}^a$	$C_1{}^a$	$\zeta_2{}^a$	$C_2{}^a$
As	4*s*	− 16.22	2.23			
	4*p*	− 12.16	1.89			
Cu	4*s*	− 11.40	2.20			
	4*p*	− 6.06	2.20			
	3*d*	− 14.00	5.95	0.5933	2.30	0.5744
Nb	5*s*	− 10.10	1.89			
	5*p*	− 6.86	1.85			
	4*d*	− 12.10	4.08	0.6401	1.64	0.5516
Ni	4*s*	− 10.95	2.10			
	4*p*	− 5.80	2.10			
	3*d*	− 13.80	5.75	0.5769	2.20	0.5938
P	3*s*	− 18.60	1.75			
	3*p*	− 14.00	1.30			
Si	3*s*	− 17.30	1.38			
	3*p*	− 9.20	1.38			
V	4*s*	− 8.81	1.30			
	4*p*	− 5.52	1.30			
	3*d*	− 11.00	4.75	0.4755	1.70	0.7052
W	6*s*	− 8.26	2.34			
	6*p*	− 5.17	2.31			
	5*d*	− 10.37	4.98	0.6685	2.07	0.5424

[a] *d*-type atomic orbitals are described by a linear combination of two STOs. ζ_1 and ζ_2 are the STO exponents, and C_1 and C_2 are the coefficients.

directions running parallel to the (001) plane are rather flat, whereas the bands associated with directions having a component along c^* are particularly dispersed. Clearly, with respect to orbital interactions W_5As_4 has a strong one-dimensional character. The total and projected DOS are shown in Fig. 5, together with the COOP curves corresponding to the major interatomic contacts in the structure. The Fermi level is situated very close to a minimum of DOS and cuts the metallic *d* band. It is interesting to note that all the COOP curves change their sign not far from the Fermi level; i.e., almost all the bonding states are occupied whereas almost all the antibonding states are vacant. In other words, the actual electron count of W_5As_4 nearly maximizes the strength of all the bonds. In order to evaluate more precisely the most favored range of electron count, we have calculated for different VECs the overlap populations of all the bonding contacts that are present in the structure. The VEC was varied in the region above and below the actual Fermi level of W_5As_4, which corresponds to VEC = 50. As said above, this energy range corresponds to the metal *d*-band. As a consequence, the W–As overlap populations are almost constant within this energy range (see also Fig. 5). Although they are large, indicating that the stability of the M_5X_4 structure is largely driven by M–X bonding, they have no significant effect on the precise value of the favored VEC counts. The overlap population corresponding to the shortest nonbonding As ⋯ As contacts is small, indicative of a very small attractive interaction and also little variance in the calculated VEC range. This result suggests that $X \cdots X$ bonding is also not involved in the tuning of the favored electron count. Consistently with the large metallic character of the states in the explored VEC range, the W–W overlap populations change significantly within this range, as exemplified by the corresponding variation curves shown in Fig. 6. The intercluster W_{II}–W_{II} bond is computed to have its maximum strength for VEC = 49, while the intracluster W_I–W_{II} and W_{II}–W_{II} bonds have the maximum strength for VEC = 48 and 46, respectively. Taking into account that in

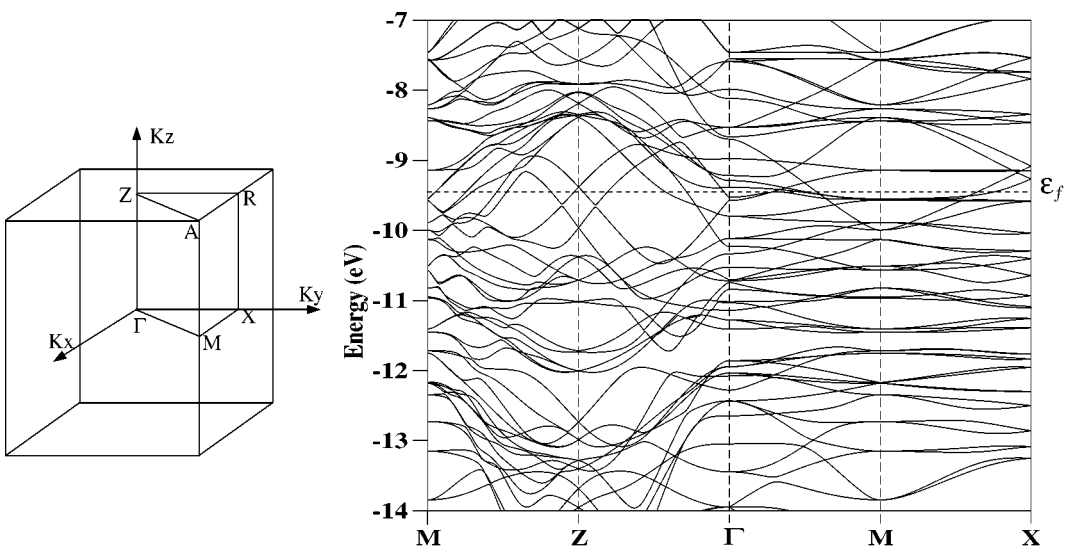

FIG. 4. Band structure of W_5As_4.

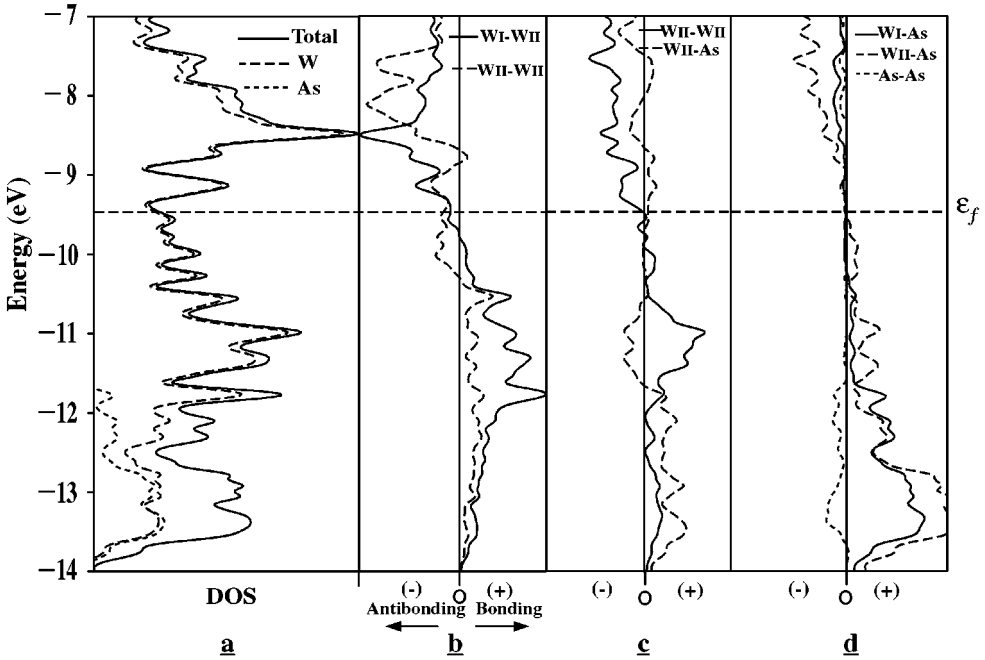

FIG. 5. DOS and COOP curves computed W_5As_4: (a) Total DOS, and W- and As-projected DOS; (b) intrachain W–W COOP curves; (c) interchain W–W and W–As COOP curves; (d) As ··· As and intrachain W–As COOP curves.

the crystal the multiplicity of the intracluster W_I–W_{II} bond is twice the multiplicity of the other W–W contacts, the average W–W overlap population is maximum for VEC = 47. Its variation is also reported in Fig. 6. It shows a flat top around its maximum in which the average W–W overlap population varies by less than 3%. This plateau corresponds to the VEC range 44–50, which incidentally is the observed VEC range for compounds adopting the Ti_5Te_4-type structure. This is consistent with the fact that the *M*–*M* bonding is the major factor governing the VEC.

BONDING ANALYSIS OF V_3As_2

The total and projected DOS and major COOP curves of V_3As_2 (VV_5As_4) are shown in Fig. 7, together with the major COOP curves. As for W_5As_4 and even more precisely, all the COOP curves change their sign almost exactly at the Fermi level, indicating that the actual electron count of VV_5As_4 maximizes the stability of such an architecture. The question which arises then is how many electrons are given (withdrawn) by (to) the inserted V atom to the V_5As_4 substructure? In other words, what is the oxidation state of the inserted atom? The environment of this atom is a distorted octahedron of arsenic. A simple extended Hückel calculation of VAs_6 "molecule" taken out of the crystal leads to the expected two-below-three level ordering of the five 3d AOs. This large splitting completely disappears in the extended structure of V_3As_2. The DOS projection on the inserted V atoms form a spread-out 3d massif that is cut by the Fermi level close to its maximum (Fig. 7a). The reason for the absence of any "t_{2g}/e_g" splitting lies in the fact that in the solid the ligand field is weaker than in an isolated VAs_6 "molecule." Indeed, there are several metal atoms competing

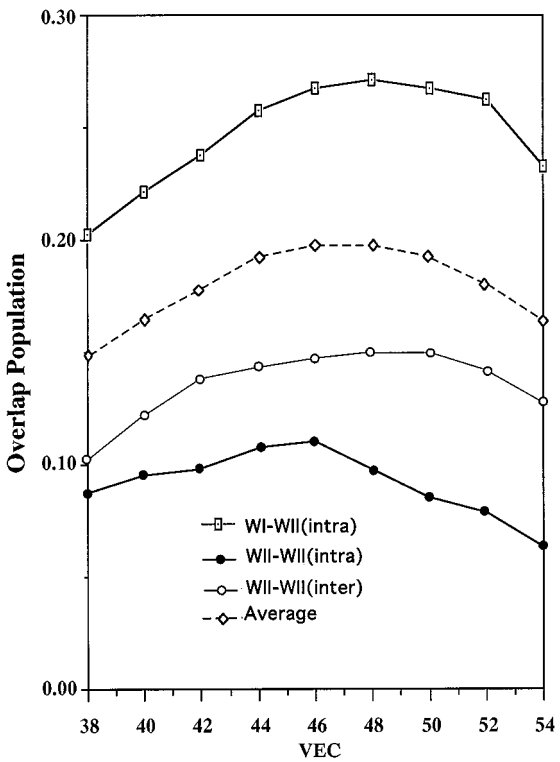

FIG. 6. Variation of the inter- and intrachain W–W overlap populations and of their weighted average with respect to VEC.

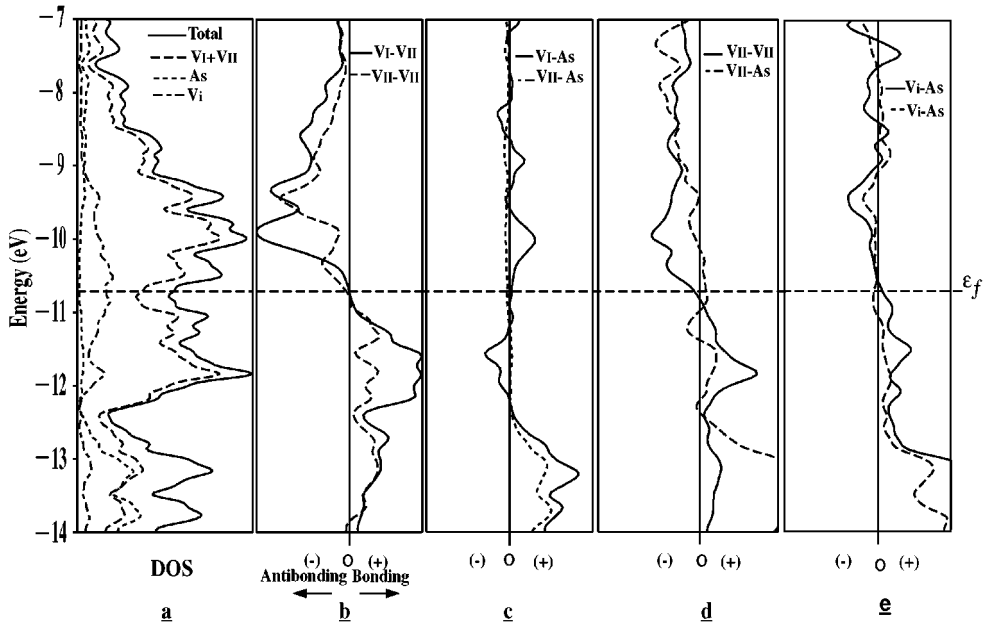

FIG. 7. DOS and COOP curves computed for V_3As_g: (a) Total DOS, and V- and As-projected DOS; (b) intrachain V–V COOP curves; (c) intrachain V–As COOP curves; (d) interchain V–V and V–As COOP curves; and (e) Vi–As COOP curves.

for each lone pair of the formally As^{-3} ligands. The number of 3d electrons occupying the *d* band of the inserted atoms is ≈ 2.5, indicative of an oxidation state close to $+2.5$. This leads to VEC = 47.5 for the $(V_5As_4)^{2.5-}$ substructure in V_3As_2 (VV_5As_4), a value situated in the predicted VEC range for the Ti_5Te_4-type structure (see above). Therefore, the role of the inserted V atoms is to provide to the V_5As_4 substructure with some electrons in order to approach its ideal VEC count and also to stabilize the whole V_3As_2 arrangement in making additional V–As bonds.

BONDING ANALYSIS OF $Cu_4Nb_5Si_4$

The total and projected DOS and the major COOP curves of $Cu_4Nb_5Si_4$ are shown in Fig. 8. As for the compounds, the COOP curves associated with the bonds of the Nb_5Si_4 substructure change their sign close to the Fermi level, suggesting that the actual electron count is very close to that which provided this substructure with the best stability.

The computed Cu–Cu overlap populations (0.035 and 0.037) are small, as compared to the intracluster Nb–Nb

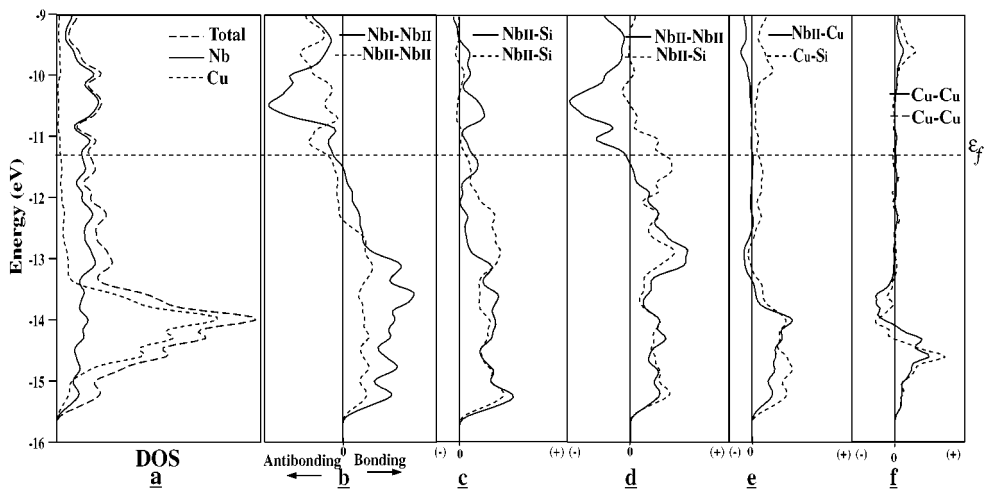

FIG. 8. DOS and COOP curves computed for $Cu_4Nb_5Si_4$: (a) Total DOS and Nb- and Cu-projected DOS; (b) intrachain Nb–Nb COOP curves; (c) intrachain Nb–Si COOP curves; (d) interchain Nb–Nb and Nb–Si COOP curves; (e) Nb–Cu and Cu–Si COOP curves; and (f) Cu–Cu COOP curves.

values (0.283 and 0.124). They are consistent with the existence of weak d^{10}–d^{10} bonding (21). As a matter of fact, the DOS projection on the inserted Cu atoms clearly shows an occupied 3d band centered around -14.5 eV. Clearly the oxidation state of Cu is $+1$. This leads to VEC $= 45$ for the $(Nb_5Si_4)^{4-}$ substructure in $Cu_4Nb_5Si_4$. The Cu^I atoms lie in a distorted trigonal planar environment of As atoms, a rather common coordination mode for d^{10} metals. Additional d^{10}–d^{10} bonding between the copper atoms contributes to the stabilization of the chains of fused Cu^I tetrahedra. Previous calculations on the isostructural $Ni_4Nb_5P_4$ compound lead to a similar description with chains of Ni^0 (d^{10}) tetrahedra inserted into a 45-VEC Nb_5P_4 matrix (11).

CONCLUSION

The VEC counts of all the characterized M_5X_4 compounds adopting the Ti_5Te_4-type structure lie in the range 44–50. Our calculations indicate that the major factor governing the VEC is M–M bonding. This bonding is computed to be almost constant and maximum in the same VEC range 44–50. Therefore, it is unlikely that new compounds adopting the Ti_5Te_4-type structure would have a VEC situated outside of this range. For a particular compound, the choice for a particular VEC inside the range 44–50 results from a compromise between the various M–M and M–X bond strengths, and, of course, electroneutrality.

When the octahedral voids located between the chains are occupied by extra metal atoms, such as in V_3As_2 (VV_5As_4), it provides the M_5X_4 substructure with an electron number which tends to maximize its M–M bonding. A similar situation occurs in $M'_4M_5X_4$ compounds when the voids are occupied by chains of edge-sharing M'_4 tetrahedra. In this case, the electron transfer to the M_5X_4 substructure (if any) is such that the oxidation state corresponds to a d^{10} configuration for M'. The M' atoms are attached to the structure through strong M'–X bonds and weak d^{10}–d^{10} bonding inside the chains of edge-sharing M'_4 tetrahedra.

ACKNOWLEDGMENTS

This work was financially supported by a French–Morrocan governemental grant (Action Intégrée 95/1012).

REFERENCES

1. F. Charki, S. Députier, P. Bénard-Rocherullé, R. Guérin, and E. H. El Ghadraoui, *J. Solid State Chem.* **131,** 310 (1997).
2. F. Gronvold, A. Kjekshus, and F. Raaum, *Acta Crystallogr.* **14,** 930 (1961).
3. D. Eberle and K. Schubert, *Z. Metallkd.* **59,** 306 (1968).
4. F. Gronvold, H. Haraldsen, P. Pedersen, and T. Tufte, *Rev. Chim. Minér.* **6,** 215 (1969).
5. E. Röst and L. Gjertsen, *Z. Anorg. Allg. Chem.* **328,** 300 (1964).
6. S. Furuseth and A. Kjekshus, *Acta Chem. Scand.* **18,** 1180 (1964).
7. K. Selte and A. Kjekshus, *Acta Chem. Scand.* **17,** 2560 (1963).
8. S. Furuseth and A. Kjekshus, *Acta Chem. Scand.* **19,** 95 (1965).
9. P. Jensen and A. Kjekshus, *Acta Chem. Scand.* **20,** 1309 (1966).
10. R. Berger, *Acta Chem. Scand. A* **31,** 287 (1981).
11. F. Charki, S. Députier, P. Bénard-Rocherullé, R. Guérin, M. Bouayed, A. Le Beuze, and J.-Y. Saillard, *Solid State Sci.* **1,** 607 (1999).
12. R. Berger, P. Phavanantha, and M. Mongkolsuk, *Acta Chem. Scand.* **134,** 77 (1980).
13. E. Ganglberger, *Monatsh. Chem.* **99,** 549 (1968).
14. R. Hoffmann and W. N. Lipscomb, *J. Chem. Phys.* **36,** 79 (1962).
15. R. Hoffmann, *J. Chem. Phys.* **39,** 1397 (1963).
16. M.-H. Whangbo and R. Hoffmann, *J. Am. Chem. Soc.* **100,** 6093 (1978).
17. M.-H. Whangbo, R. Hoffmann, and R. B. Woodward, *Proc. R. Soc. A* **366,** 23 (1979).
18. G. A. Landrum, "Yet Another Extended Hückel Molecular Orbital Package." *YAeHMOP*. Cornell University, 1997. [YAeHMOP is freely available at http://overlap.chem.cornell,edu:8080/yaehmop.html.]
19. R. Hoffmann, "Solids and Surfaces. A Chemist's View of Bonding in Extended Structures." VCH, New York, 1988.
20. C. Mealli and D. M. Proserpio, *J. Chem. Educ.* **67,** 399 (1990).
21. P. K. Mehrota and R. Hoffmann, *Inorg. Chem.* **17,** 2187 (1978).